STATE OF THE CLIMATE IN 2018

Special Supplement to the
Bulletin of the American Meteorological Society
Vol. 100, No. 9, September 2019

Table 4.2. Global counts of tropical cyclone activity by basin for 2018. Bold indicates ≥ top quartile from 1981–2010 based on Schreck et al. (2014) and italics indicate ≤ bottom quartile. Please note that some inconsistencies between Table 4.2 and the text of the various basin write-ups in Section f exist and are unavoidable, as the tallying of the global TC numbers is challenging and involves more than simply adding up basin totals, because some storms cross TC basin boundaries, some TC basins overlap, and multiple agencies are involved in tracking and categorizing TCs.

Basin	TCs	HTCs	Major HTCs	SS Cat 5	ACE ($\times 10^4$ kt^2)
North Atlantic	**15**	**8**	2	1	133
Eastern North Pacific	**23**	**13**	**10**	**3**	**316**
Western North Pacific	28	16	9	**6**	341
North Indian	**8**	**4**	**1**	0	**31**
South Indian	*6*	**7**	3	0	85
Australian	10	*3*	*1*	**1**	*46*
Southwest Pacific	5	3	1	0	50
Totals	**95**	**54**	**27**	**11**	**1002**

more than in 2016 (Diamond and Schreck 2017, 2018), and second only to 1997 when there were 12. The 11 Category 5 storms were: (a) Super Typhoons Yutu, Mangkhut, Maria, Trami, Jebi, and Kong-Rey in the western North Pacific; (b) Hurricanes Lane, Walaka, and Willa in the eastern North Pacific; (c) Severe TC Marcus in the Australian basin; and (d) Hurricane Michael in the North Atlantic.

Sidebars 4.1 and 4.2 detail the record-setting and devastating local impacts of Hurricane Michael, a rare landfalling Category 5 storm that developed rapidly and devastated portions of the Florida Panhandle and southern Georgia.

2) Atlantic basin—G. D. Bell, E. S. Blake, C. W. Landsea, H. Wang, S. B. Goldenberg, and R. J. Pasch

(i) 2018 seasonal activity

The 2018 Atlantic hurricane season produced 15 named storms, including 8 hurricanes, 2 of which became major hurricanes (Fig. 4.17a). The HURDAT2 1981–2010 seasonal averages (included in IBTrACS) are 11.8 named storms, 6.4 hurricanes, and 2.7 major hurricanes (Landsea and Franklin 2013). The 2018 seasonal ACE value (Bell et al. 2000) was nearly 145% of the 1981–2010 median (which is 92.4×10^4 kt^2; Fig. 4.17b). This value is above NOAA's threshold for an above-normal season (120%), and the numbers of named storms and hurricanes were also both above average. Therefore, NOAA classifies the 2018 season as above normal, making 2018 the third consecutive above-normal season, and the 16th above-normal season (of 24) since the current Atlantic high-activity

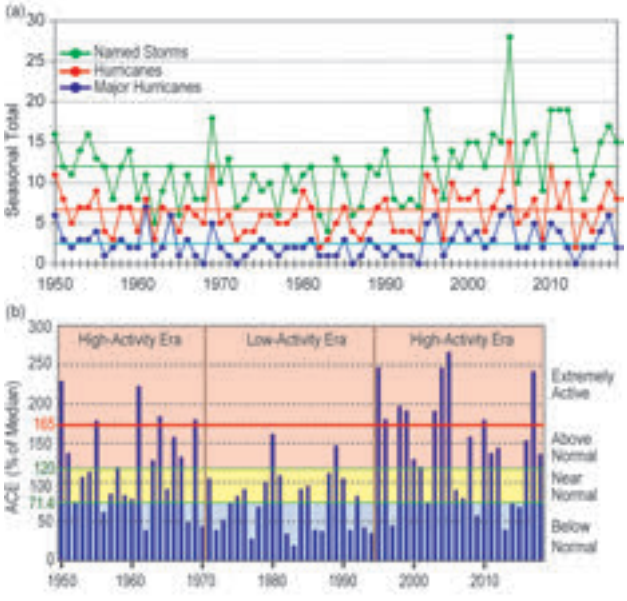

Fig. 4.17. Seasonal Atlantic hurricane activity during 1950–2018 based on HURDAT2 (Landsea and Franklin 2013). (a) Number of named storms (green), hurricanes (red), and major hurricanes (blue), with 1981–2010 seasonal means shown by solid colored lines. (b) ACE index expressed as a percent of the 1981–2010 median value. Red, yellow, and blue shadings correspond to NOAA's classifications for above-, near-, and below-normal seasons. Thick red horizontal line at 165% ACE value denotes the threshold for an extremely active season. Vertical brown lines separate high- and low-activity eras. Note: there is a low bias in activity during the 1950s to the early 1970s due to the lack of satellite imagery and the associated Dvorak technique used to interpret TC intensity for systems over the open ocean.

era began in 1995 (Landsea et al. 1998; Goldenberg et al. 2001). The previous Atlantic high-activity era of 1950–70 also featured numerous above-normal seasons (10 of 21), while the intervening low-activity era of 1971–94 had only 2 of 24 (Bell et al. 2018). Note that reliable basin-wide records for exact season-to-season comparisons with ACE began in the mid-1970s with the advent of the geostationary satellite era (Landsea et al. 2006).

(ii) Storm formation regions, tracks, and landfalls

The vast majority of Atlantic tropical storms and hurricanes develop during the peak months of the season (August–October, ASO). During 2018, 12 of the 15 named storms formed during ASO, accounting for 6 of the 8 hurricanes, including both major hurricanes (Fig. 4.18a,b).

The activity was focused in two main regions. One was the Main Development Region (MDR), which spans the tropical Atlantic Ocean and Caribbean Sea between 9.5°N and 21.5°N (green box, Fig. 4.18a) (Goldenberg and Shapiro 1996; Goldenberg et al. 2001; Bell and Chelliah 2006). The other was located north of the MDR across the western and central subtropical North Atlantic.

Above-normal seasons typically have far more activity in the MDR compared to near-normal and below-normal seasons (Bell and Chelliah 2006; Bell et al. 2017, 2018). In 2018, eight of the 15 named storms formed in the MDR, resulting in five hurricanes, two of which were major. These eight TCs accounted for 66% of the seasonal ACE total. Six of these eight TCs, including four hurricanes and one major hurricane, formed over the eastern tropical Atlantic, while nearly the entire western half of the MDR (west of 50°W) was devoid of hurricanes.

Consequently, although the 2018 MDR activity was substantial, it was fairly modest for an above-normal season. For example, the numbers of MDR-spawned named storms, hurricanes, and major hurricanes were all lower than the 1981–2010 above-normal season averages of 9.3 named storms, 6.8 hurricanes, and 4.2 major hurricanes, respectively. Also, the MDR-spawned ACE was only 95% of its median, well below the 120% threshold for an above-normal season. Historically, the MDR-spawned ACE has exceeded 120% in two-thirds (19 of 28) of above-normal seasons since 1950. Further comparison to past above-normal seasons indicates that the 2018 MDR-spawned ACE was the sixth lowest since 1950, and the third lowest (after 2012 and 2001) since the geostationary satellite era began in 1974. The number of MDR-spawned major hurricanes was the second lowest (after 2012).

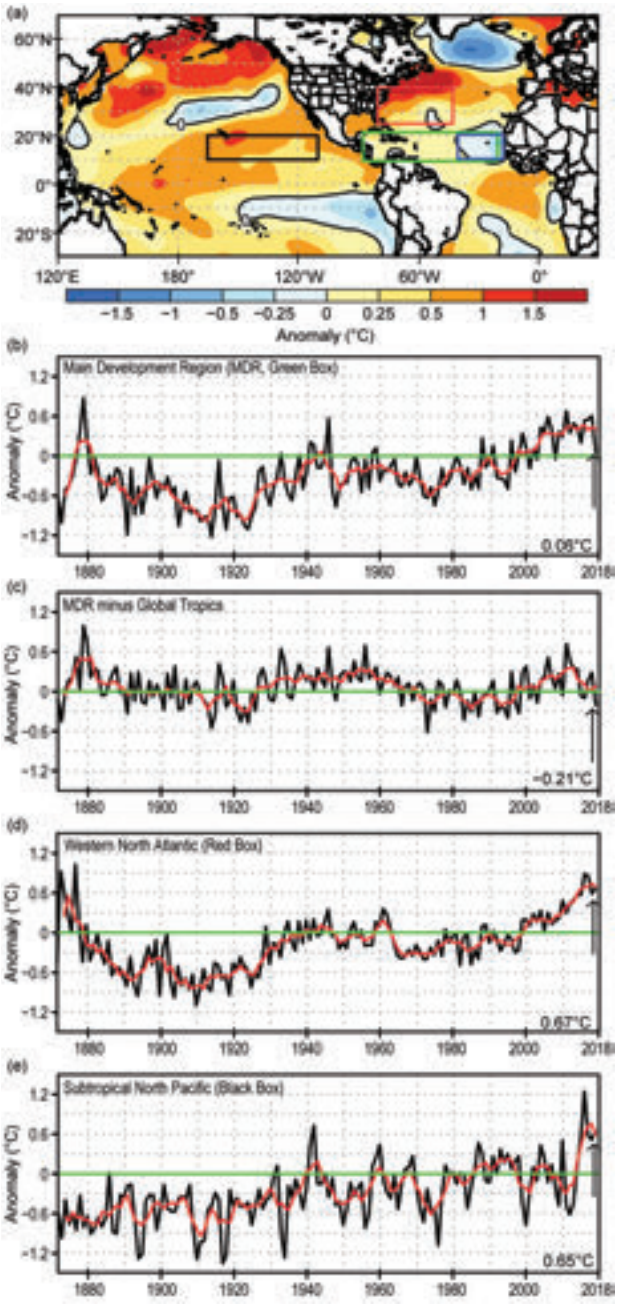

Fig. 4.18. (a) Aug–Oct 2018 SST anomalies (°C). (b)–(e) Time series of Aug–Oct area-averaged SST anomalies (°C, black) and 5-pt. running mean of the time series (red) in (b) the MDR [green box in (a) spanning 19.5°–21.5°N and 20°–87.5°W], (c) difference between the MDR and the global tropics (20°N–20°S), (d) the western North Atlantic [red box in (a) spanning 25°–40°N and 42.5°–80°W], and (e) the subtropical North Pacific [black box in (a) spanning 10°–20°N and 165°–110°W]. The blue box in (a) denotes the eastern MDR. Data source is ERSSTv5 (Huang et al. 2017). Anomalies are departures from the 1981–2010 period means.

In contrast, near-record TC activity was observed during 2018 across the western and central subtropical North Atlantic (north of 21.5°N). This activity pushed the season into the above-normal category for the total basin. Six named storms formed in this region, with three becoming hurricanes. These six TCs accounted for 32% of the seasonal total. For above-normal seasons, this is the third highest ACE produced by TCs forming north of the MDR since 1950 (following 119% in 2005 and 48% in 1954). Five of these six TCs, including two hurricanes, developed initially as subtropical storms. In all, there were a record seven subtropical storms during 2018, breaking the previous record of five set in 1969.

Four TCs during 2018 made landfall in the continental United States, two as tropical storms and two as hurricanes. The first was Tropical Storm Alberto in northwestern Florida on 28 May. The second was Hurricane Florence, which made landfall in North Carolina on 14 September as a Category 1 hurricane and subsequently produced catastrophic flooding across portions of North and South Carolina. The third U.S. landfalling TC of 2018 was Tropical Storm Gordon in southwestern Alabama on 5 September. The fourth was Hurricane Michael, which developed over the northwestern Caribbean Sea on 8 October and made landfall on the Florida Panhandle in Mexico Beach, Florida, two days later. Michael had Category 5 maximum sustained winds of 140 kt (69 m s^{-1}) at landfall and was the strongest TC to strike the Panhandle, and was the fourth strongest for any continental U.S. hurricane landfall on record since accurate records began in the late 1800s. For the continental United States, Michael was the strongest landfalling TC since Hurricane Andrew in 1992.

(iii) Sea surface temperatures

There were five main SST signals during ASO 2018 (Fig. 4.18). The first was near-average SSTs across the MDR (Fig. 4.18a), with most areas having departures within ± 0.25°C of average. For the MDR as a whole, the area-averaged SST anomaly was +0.06°C, the lowest value since 2009 (Fig. 4.18b).

The second signal was that the MDR average SST anomaly during this period was 0.21°C lower than the remainder of the global tropics (Fig. 4.18c). A relatively cool MDR of this magnitude has not been seen since the late 1990s and is more typical of the Atlantic low-activity eras (Vecchi and Soden 2007; Bell et al. 2018), such as 1971–94 and 1900–25.

The third SST signal focused on the eastern MDR (blue box, Fig. 4.18a), where a pronounced increase of temperature anomalies occurred during August. As a result, the ASO area-averaged SST anomaly in this region (−0.18°C) was much higher than the June–July anomaly of −0.82°C (not shown). These more moderate SST anomalies made the eastern MDR increasingly hospitable to TC activity.

The fourth signal reflected near-record high SSTs during ASO in the western and central North Atlantic (red box, Fig. 4.18a), where as noted above, near-record TC activity was observed in 2018. The area-averaged SST anomaly in this region (+0.67°C) was comparable to the warmest ASO period in the 1871–2018 record (Fig. 4.18d).

The fifth SST signal reflected near-record anomalous warmth (Fig. 4.18e) across the subtropical North Pacific (black box, Fig. 4.18a). Since 2015, this region has experienced exceptionally high SSTs not seen previously since the early 1940s. During 2018, this warmth was accompanied by a progressive warming of the central and east-central equatorial Pacific, with area-averaged SST anomalies reaching +0.7°C during SON as measured by the ENSO-related ONI (see Fig. 4.1).

(iv) Atmospheric conditions

The 2018 Atlantic hurricane season was remarkable for being above normal despite strong westerly vertical wind shear (generally 12–16 m s^{-1}) across the western and central MDR (blue box, Figs. 4.19a,b). The area-averaged shear in this region was 13.7 m s^{-1} during ASO (Fig. 4.19c), the strongest since the mid-1980s. This shear pattern reflected enhanced upper-level (200-hPa) westerly winds within the base of an amplified Tropical Upper Tropospheric Trough (TUTT; Fig. 4.20a). These overall conditions are typical of less active seasons (Bell and Chelliah 2006).

The enhanced upper-level westerlies and shear were related in part to an extensive pattern of anomalous upper-level divergence (Fig. 4.21a) and enhanced tropical convection (indicated by negative OLR anomalies, Fig. 4.21b) across the central and eastern subtropical North Pacific (black box, Figs. 4.21a,b). These conditions are known to increase the upper-level westerlies, and hence the vertical wind shear, in the western MDR (Klotzbach 2010). During August–September 2018, the area-averaged OLR anomaly in the subtropical North Pacific region was the third most negative in the 1979–present record (bars, Fig. 4.21c), suggesting there was sufficient forcing to negatively impact the Atlantic hurricane season. These conditions were associated with a northward shift and strengthening of the Pacific ITCZ, with near-record warm SST anomalies across the region (Fig. 4.18e) and the most active eastern-

central North Pacific hurricane season on record (as measured by ACE).

Anomalous convection across the subtropical North Pacific during August–September also has an inverse relationship with ENSO phase (i.e., the ONI) but not necessarily with the specific strength of the El Niño and La Niña episodes. Looking at SON ONI values during 1979–2018, roughly half of those years with ONI ≥ +0.5°C (typically El Niño) featured enhanced convection with negative OLR anomalies of more than −0.5 standard deviations across the subtropical North Pacific (Fig. 4.22a). Conversely, about two-thirds of years with an ONI ≤ −0.5°C (typically La Niña) featured suppressed convection with positive OLR anomalies exceeding +0.5 standard deviations in that region. This inverse relationship is also seen by looking at August–September periods when

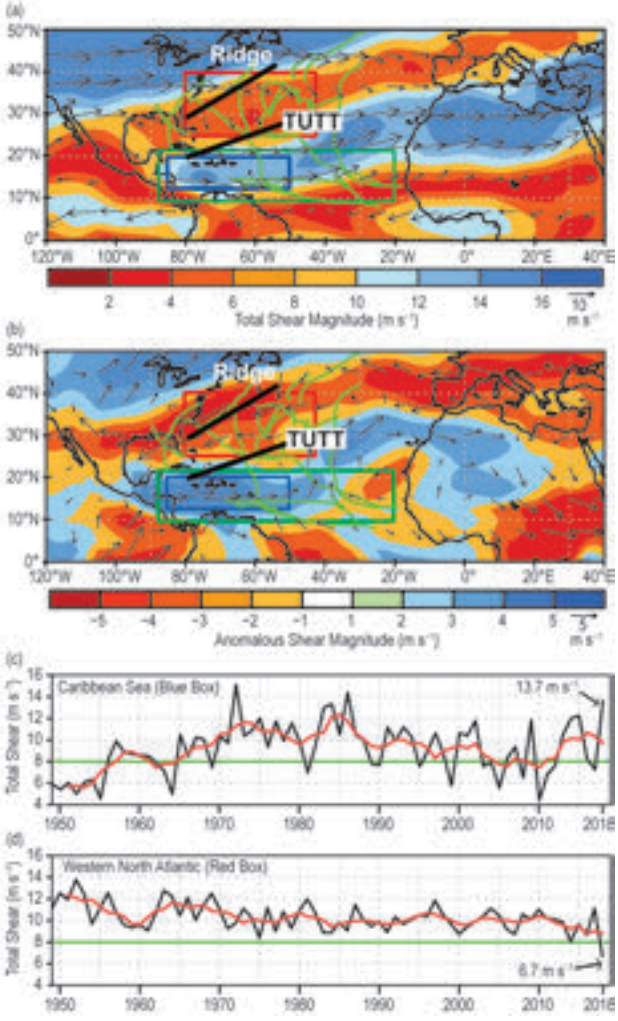

Fig. 4.19. Aug–Oct 2018, 200–850 hPa magnitude of vertical wind shear (m s^{-1}): (a) total magnitude (shaded, m s^{-1}) and (b) anomalous magnitude (shaded, m s^{-1}). (c),(d) Time series of ASO vertical shear magnitude (black) and 5-pt. running mean of the time series (red) averaged over (c) the western MDR [blue box in (a) spanning 12.5°–20°N and 85°–50°W] and (d) the western North Atlantic [red box in (a) spanning 25°–40°N] and 80°–42.5°W. In (a), (b), the upper-level ridge and TUTT discussed in the text are labeled and denoted by thick black lines. The 2018 TC tracks (green lines) are shown, the vector scale (m s^{-1}) is below right of color bar. Green box denotes the MDR. Data are from NCEP–NCAR reanalysis (Kalnay et al. 1996). Anomalies are departures from 1981–2010 means.

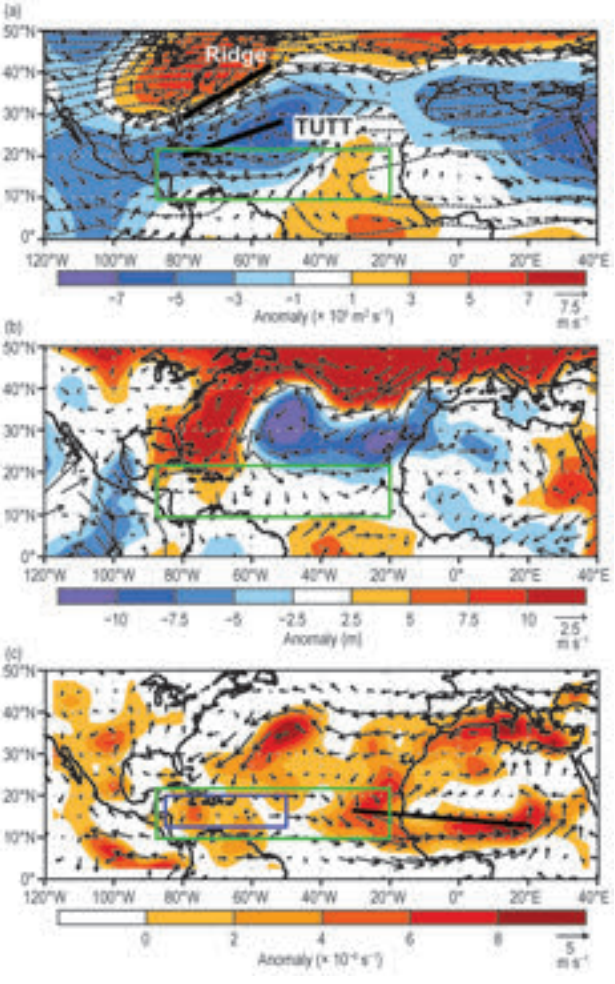

Fig. 4.20. Aug–Oct 2018: (a) 200-hPa total streamfunction (contours, interval is 5 × 10^6 m^2 s^{-1}) and anomalies (shaded); (b) anomalous 1000-hPa heights (shaded, m); and (c) anomalous 700-hPa cyclonic relative vorticity (shaded, × 10^{-6} s^{-1}) and vector winds. The corresponding anomalous wind vectors (m s^{-1}) are shown in each panel. In (a) the upper-level ridge and TUTT discussed in the text are labeled and denoted by thick black lines. In (c) the thick solid line indicates the axis of the mean African Easterly Jet, which was hand-drawn based on total seasonal wind speeds (not shown). Vector scales differ for each panel and are below right of color bar. Green box denotes the MDR. Anomalies are departures from 1981–2010 means. [Source: NCEP–NCAR reanalysis (Kalnay et al. 1996).]

convection was most anomalous (OLR anomalies exceeding ±1 standard deviations) across the subtropical North Pacific. The SON ONI values were at least +0.5°C (as in 2018) in two-thirds of years when the convection was most enhanced, and below at least −0.5°C in two-thirds of years when the convection was most suppressed (Fig. 4.22b).

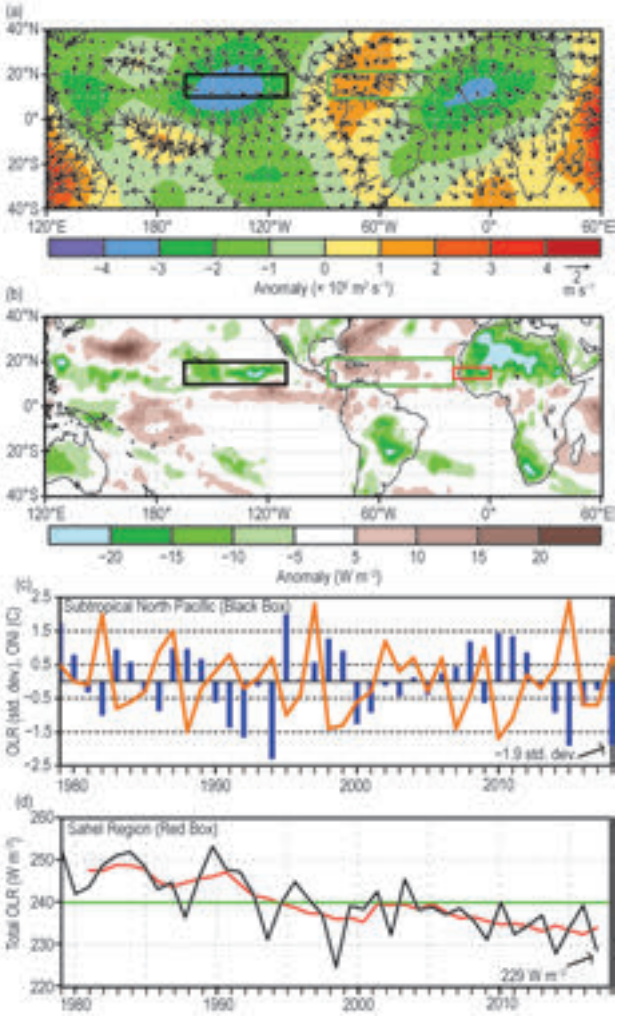

Fig. 4.21. Aug–Sep 2018: (a) anomalous 200-hPa velocity potential (× 10^6 m^2 s^{-1}) and divergent wind vectors (m s^{-1}) and (b) anomalous OLR (W m^{-2}), with negative (positive) values indicating enhanced (suppressed) convection. (c) SON ONI (red line) overlaid with time series of Aug–Sep area-averaged OLR anomaly (blue bars) over the subtropical North Pacific [black box in (a),(b) spanning 10°–20°N and 165°–110°W]. (d) Time series of Aug–Sep area-averaged total OLR (black) and 5-pt. running mean of the time series (red) over the African Sahel region [red box in (b) spanning 12.5°–17.5°N and 20°W–0°]. Green box in (a),(b) denotes the Atlantic MDR. OLR data are based on AVHRR (Liebmann and Smith 1996). Velocity potential and wind data are from NCEP–NCAR reanalysis (Kalnay et al. 1996). Anomalies are departures from the 1981–2010 means.

Given the above conditions, the question then arises as to why the 2018 Atlantic hurricane season was above normal. One main reason was the numerous tropical storms and hurricanes (including Hurricane Florence) across the central/western subtropical North Atlantic that formed in response to exceptionally conducive wind and air pressure patterns in that region (Figs. 4.19, 4.20, 4.23). In the upper troposphere, these conditions included a ridge in the 200-hPa streamfunction field that extended across the eastern United States and western North Atlantic, and also across the central North Atlantic mainly between 40°–50°N (Fig. 4.20a). The amplified TUTT was located farther south. The corresponding height anomaly pattern extended down to the ocean surface, as seen in both the lower (1000-hPa; Fig. 4.20b) and middle (500-hPa; Fig. 4.23a) troposphere.

This overall pattern was associated with a northward shift of the jet stream and anomalously weak upper-level westerly winds (indicated by easterly and northeasterly wind anomalies; Fig. 4.20a) and exceptionally weak vertical wind shear (red box, Figs. 4.19a,b) from the eastern United States to the central

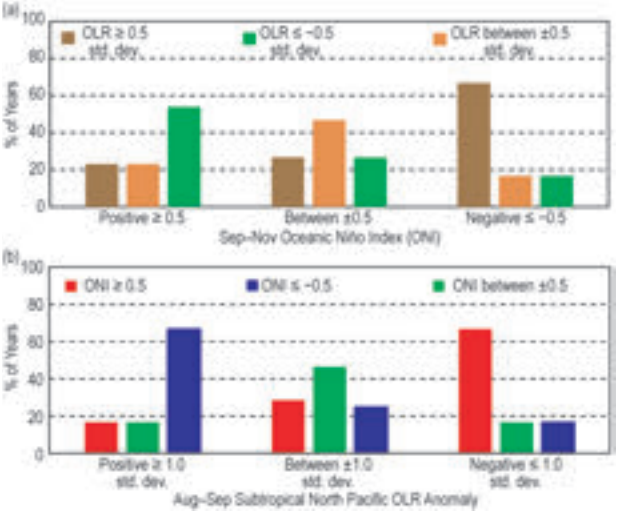

Fig. 4.22. (a) For each ENSO phase during Sep–Nov as measured by the ONI, the bars show the percent of years in which the area-averaged OLR anomaly during Aug–Sep in the subtropical North Pacific region (blue box, Figs. 4.23a,b) was positive (≥ +0.5 std. dev.), average (within ± 0.5 std. dev), and negative (≤ +0.5 std. dev). (b) For each range of standardized OLR anomalies (Liebmann and Smith 1996) during Aug–Sep in the subtropical North Pacific region, the bars show the percent of years in which the ONI during Sep–Nov was positive (≥ +0.5, El Niño like), average (within ± 0.5, ENSO-neutral), and negative (≤ +0.5, La Niña-like). Negative (positive) OLR anomalies indicate enhanced (suppressed) convection, and are associated with stronger (weaker) vertical wind shear in the western MDR.

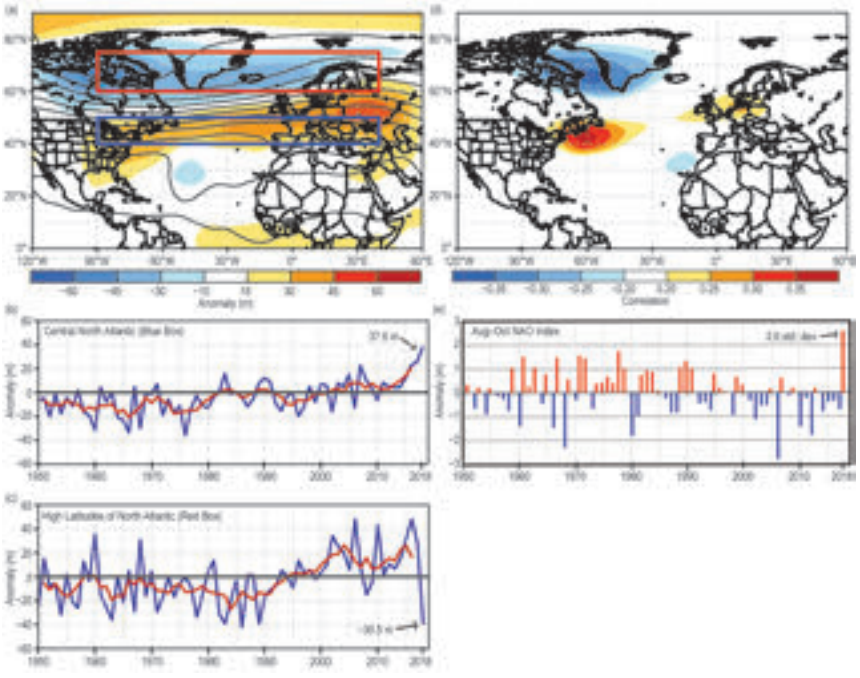

Fig. 4.23. ASO 2018: (a) 500-hPa conditions: height (m, solid lines, interval is 60 m) and anomalies (m, shaded). (b),(c) Time series of height anomalies (m, black) and 5-pt. running mean of the time series (red) averaged over (b) the central North Atlantic [blue box in (a) spanning 40°–50°N and 90°W–40°E], and (c) the high latitudes of the North Atlantic [red box in (a) spanning 60°–75°N and 90°W–40°E]. (d) 1950–2018 correlation (× 100) loading pattern of the NAO, and (e) time series of the 500-hPa NAO index. NAO loading pattern and time series are obtained from the NOAA Climate Prediction Center (www.cpc.ncep.noaa.gov/data/teledoc/telecontents.shtml). Data are from NCEP–NCAR reanalysis (Kalnay et al. 1996). Anomalies are departures from the 1981–2010 means.

North Atlantic. The area-averaged magnitude of the vertical wind shear in this region was 6.7 m s^{-1}, dropping below 8 m s^{-1} for the first time in the ASO 1950–2018 record (Fig. 4.19d). On monthly time scales, shear values less than 8 m s^{-1} are considered conducive to hurricane formation (Bell et al. 2017).

Further inspection of the 500-hPa height anomaly field shows that these conducive ASO conditions were associated with a record-strength, larger-scale circulation pattern in the extratropics (Fig. 4.23). This pattern featured record positive height anomalies across the central North Atlantic, with area-averaged values nearly double the previous high (Fig. 4.23b). The pattern also featured near-record negative height anomalies across the high latitudes of the North Atlantic (Fig. 4.23c). This north–south dipole pattern reflected the strongest positive phase of the North Atlantic Oscillation (NAO, Fig. 4.23d) for the ASO season from 1950–present (Fig. 4.23e).

Another major contributing factor to the above-normal 2018 Atlantic hurricane season was conducive conditions in the eastern MDR, which resulted in six named storms with four being hurricanes and one being a major hurricane. Atmospheric conditions in this region included weaker easterly trade winds (indicated by westerly wind anomalies) that extended upward to at least the 700-hPa level (Figs. 4.20b,c), the approximate level of the African Easterly Jet (AEJ). This anomaly pattern had two main impacts. First, it helped to return anomalously cold SSTs during June–July in the eastern MDR toward near-average levels. Second, it contributed to a deep layer of anomalous cyclonic relative vorticity (i.e., increased cyclonic shear) along the equatorward flank of the AEJ (shading, Fig. 4.20c). These conditions are known to help maintain African easterly waves and to provide an inherent cyclonic rotation to their embedded convective cells (Bell et al. 2004, 2006, 2017, 2018).

Historically, these wind patterns reflect enhanced low-level inflow into a stronger West African monsoon (Gray and Landsea 1992; Hastenrath 1990; Landsea et al. 1992; Bell and Chelliah 2006; Bell et al. 2018). The peak months of that monsoon season are July–September. At 200 hPa, one indicator of an enhanced monsoon during August–September 2018 was an extensive area of anomalous upper-level divergence across western Africa, along with its associated core of negative velocity potential anomalies (Fig. 4.21a). Another indicator was enhanced convection (shown by negative OLR anomalies) in the African Sahel region (red box, Fig. 4.21b). The total area-averaged OLR in this region during August–September was 229 W m^{-2}, the third lowest value in the 1979–2018 record (Fig. 4.21d). In the tropics, total OLR values below 240 W m^{-2} indicate deep convection. The conducive hurricane conditions in the eastern MDR during ASO 2018 were linked to a northward extension of deep tropical convection across much of the Sahel region, in association with a significantly enhanced West African monsoon.

These conditions are consistent with the strong climate link that occurs on multidecadal time scales between Atlantic hurricane activity and the strength of the West African monsoon (Bell and Chelliah 2006). Specifically, the current Atlantic high-activity era (Fig. 4.17b) has featured an enhanced monsoon with total OLR values below 240 W m^{-2} in the Sahel region, whereas the low-activity period of the 1980s and early 1990s featured a weaker monsoon with OLR values in the Sahel region often well above 240 W m^{-2} (Fig. 4.21d). These multidecadal fluctuations in monsoon strength coincide with opposing phases (warm and cold, respectively) of the Atlantic Multidecadal Oscillation (AMO; Enfield and Mestas-Nuñez 1999; Bell and Chelliah 2006).

SIDEBAR 4.1: HURRICANE MICHAEL: A FLORIDA PANHANDLE RECORD-BREAKING LANDFALL—P. J. KLOTZBACH

The 2018 Atlantic hurricane season was perhaps best known for two significant hurricanes—Florence and Michael—that brought death and destruction to the continental United States. This sidebar focuses on Michael, which was first named on 7 October and became only the fourth continental U.S. landfalling Category 5 hurricane on record just three days later (Beven et al. 2019). Michael's meteorological history is discussed, followed by a discussion of the many meteorological records the storm set in its relatively short lifetime. Historical landfall records from 1851–present are taken from the National Hurricane Center/Atlantic Oceanographic and Meteorological Laboratory archive located at: www.aoml.noaa.gov/hrd/hurdat/All_U.S._Hurricanes.html.

Michael was first noted as a potential TC on 6 October. The tropical disturbance that spawned Michael brought heavy rainfall to Central America and resulted in 15 fatalities. Michael's initial development was hampered by strong vertical wind shear from an upper-level trough located in the Gulf of Mexico. However, despite continuing to encounter relatively strong vertical wind shear, Michael intensified into a tropical storm the following day. While statistical and dynamical model guidance called for relatively slow strengthening due to persistent westerly vertical wind shear from the upper-level trough in the central Gulf of Mexico, Michael deepened much faster than anticipated, reaching hurricane strength less than 24 hours after being named. Michael's intensification despite persistent wind shear may have been due to the trough in the central Gulf of Mexico generating upper-level difluence that somewhat counteracted the strong shear. In addition, another upper-level trough to the east of Michael likely aided its upper-level outflow (Beven et al. 2019). While Michael's peak rapid intensification rate never exceeded 40 kt (21 m s^{-1}) 24 h^{-1}, it intensified at a rate of 20–40 kt (10–21 m s^{-1}) 24 h^{-1} from the time that it was named until the time it made landfall near Mexico Beach, Florida.

While the dynamic environment in the western Caribbean was only marginal for Michael's development, the thermodynamic environment was much more conducive than normal. SSTs averaged 1°–2°C warmer than normal, with anomalously high levels of upper ocean heat content along Michael's track (see Fig. SB4.3). Vertical wind shear impinging on Michael also weakened considerably as the storm tracked northward from the western Caribbean into the Gulf of Mexico.

As noted earlier, Michael underwent moderate-to-rapid intensification throughout its lifetime as a named storm, reaching major hurricane strength on 9 October. Unlike most recent major hurricanes making landfall along the northern Gulf Coast that weakened in the 24 h prior to landfall (e.g., Rita and Katrina 2005; Ivan 2004; Opal 1995), Michael continued to intensify up until its landfall in Florida (Fig. SB4.1). Michael's landfall intensity of 140 kt was the fourth strongest for any continental U.S. hurricane landfall on record (since 1851), trailing in order from the strongest: Labor Day (1935), Camille (1969), and Andrew

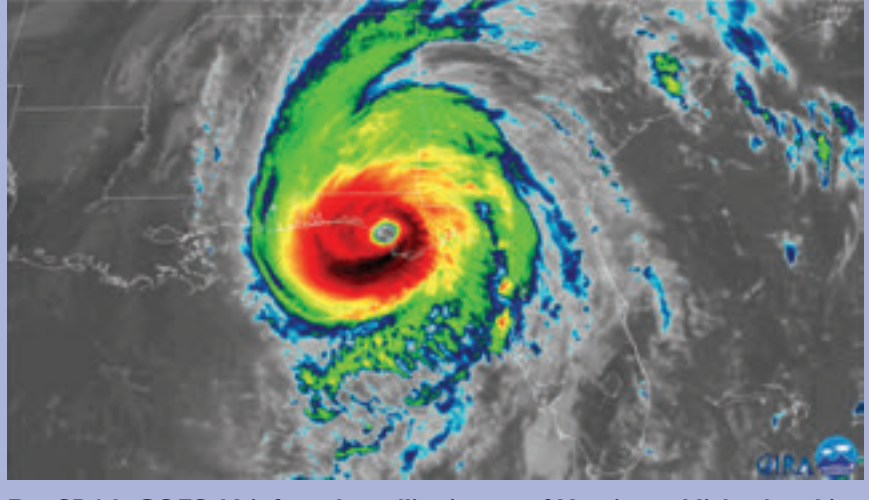

Fig. SB4.1. GOES-16 infrared satellite image of Hurricane Michael making landfall at 1800 UTC on 10 Oct (from RAMMB CIRA; http://rammb.cira.colostate.edu/).